

ORIGINAL ARTICLE

Genomic analyses reveal global functional alterations that promote tumor growth and novel tumor suppressor genes in natural killer-cell malignancies

J Iqbal^{1,9}, C Kucuk^{1,9}, RJ deLeeuw², G Srivastava³, W Tam⁴, H Geng⁵, D Klinkebiel⁶, JK Christman⁶, K Patel¹, K Cao⁵, L Shen³, K Dybkaer⁷, IFL Tsui², H Ali⁵, N Shimizu⁸, WY Au³, WL Lam² and WC Chan¹

¹Department of Pathology and Microbiology, University of Nebraska Medical Center, Omaha, NE, USA; ²British Columbia Cancer Research Centre, Vancouver, British Columbia, Canada; ³Departments of Pathology and Medicine, University of Hong Kong, Hong Kong, Hong Kong; ⁴Department of Pathology, Weill Medical College of Cornell University, New York, NY, USA; ⁵Department of Computer Science, University of Nebraska at Omaha, Omaha, NE, USA; ⁶Department of Biochemistry and Molecular Biology, University of Nebraska Medical Center, Omaha, NE, USA; ⁷Department of Hematology, Aalborg Hospital, Aarhus University Hospital, Aalborg, Denmark and ⁸Medical Research Institute, Tokyo Medical and Dental University, Tokyo, Japan

Natural killer (NK)-cell malignancies are among the most aggressive lymphoid neoplasms with very poor prognosis. We performed array comparative genomic hybridization analysis on a number of NK cell lines and primary tumors to gain better understanding of the pathogenesis and tumor biology of these malignancies. We also obtained transcriptional profiles of genes residing in these regions and compared them with normal and activated NK cells. Only 30–50% of the genes residing in the gained or deleted regions showed corresponding increased or decreased expression. However, many of the upregulated genes in regions of gain are functionally important for the proliferation and growth of the neoplastic population. Genes downregulated in regions of loss included many transcription factors or repressors, tumor suppressors or negative regulators of the cell cycle. The minimal common region of deletion in 6q21 included three known genes (*PRDM1*, *ATG5* and *AIM1*) showing generally low expression. Mutations resulting in truncated *PRDM1* and changes in conserved amino-acid sequences of *AIM1* were detected. Highly methylated CpG islands 5' of *PRDM1* and *AIM1* correlated with low expression of the transcripts. Reversal of methylation by Decitabine induced expression of *PRDM1* and cell death. In conclusion, we have shown a general tumor-promoting effect of genetic alterations and have identified *PRDM1* as the most likely target gene in del6q21. *ATG5*, an essential gene for autophagy and *AIM1*, a gene implicated in melanoma, may also participate in the functional abnormalities. *Leukemia* (2009) 23, 1139–1151; doi:10.1038/leu.2009.3; published online 5 February 2009

Keywords: NK-cell lymphoma; gene expression profiles; Array CGH; *PRDM1*; *ATG5*

Introduction

The World Health Organization classification has divided natural killer (NK)-cell malignancies into two entities: aggressive NK-cell leukemia (ANKL) and extra nodal NK-cell lymphoma of nasal type (ENKL).¹ Both of these entities are characterized by an aggressive clinical course and poor survival.² NK-cell malignancies show strong geographic predilection; they are

rare in western countries but relatively frequent in East Asia, and Central and South America.³ The diagnostic characteristics of NK-cell malignancies include germline T-cell receptor and immunoglobulin gene configurations with expression of NK cell-associated markers such as CD16 and CD56, but not surface CD3.

Hematological malignancies often accumulate multiple genomic imbalances, which play a crucial role in neoplastic transformation and tumor progression due to the activation of oncogenes or inactivation of tumor suppressor genes. Only a few studies of genome-wide alterations have been published on NK-cell malignancies^{4–11} due to the rarity of this entity and the difficulty in obtaining adequate biopsy specimens. Therefore, well-characterized NK cell lines, supplemented with tumor specimens, can have an important role in the investigation of NK-cell malignancies.¹²

The newly developed array comparative genomic hybridization (aCGH) technology has much higher resolution compared with traditional CGH and allows direct mapping of aberrations to genomic sequence.¹³ Gene expression profiling (GEP) of the same samples will provide highly complementary functional information that will also facilitate the identification of candidate genes. In this study, we performed aCGH with a high-resolution tiling DNA microarray¹⁴ and examined the expression of genes residing in the aberrant chromosomal regions. The major aims of the study were to (a) determine common DNA gains and losses by aCGH and compare these alterations with those reported in the literature to validate and better define the recurring chromosomal abnormalities, (b) correlate the genomic profiles with transcriptional profiles to determine possible functional consequences of the genetic aberrations and (c) identify target genes in the minimal aberrant regions. We found that the genetic alterations caused changes in expression of many genes that cooperate to provide a general tumor-promoting effect. We have also identified *PRDM1* as the most likely target gene in del6q21 through additional mutation and methylation analysis.

Materials and methods

Cell lines and tumor specimens

The malignant NK cell lines used in this study are summarized in Supplementary Table 1. All cell lines were cultured in RPMI 1640 (Gibco-Invitrogen, CA, USA) supplemented with 10% fetal

Correspondence: WC Chan, Amelia and Austin Vickery Professor of Pathology, University of Nebraska Medical Center, 983135 Nebraska Medical Center, Omaha, NE 68198, USA.

E-mail: jchan@unmc.edu

⁹These authors contributed equally to this work.

Received 23 September 2008; revised 25 November 2008; accepted 22 December 2008; published online 5 February 2009

calf serum, penicillin G (100 units/ml) and streptomycin (100 µg/ml), and 5–7 ng/ml interleukin (IL)-2 (R&D Bioscience, CA, USA) at 37 °C in 5% CO₂.

In addition to the cell lines, seven patients diagnosed with NK-cell malignancies were included in the study. The institutional review board of the University of Nebraska Medical Center approved this study.

Whole-genome tiling path array-based CGH

High molecular weight DNA was extracted from cell lines and tumor specimens with the standard phenol–chloroform method.¹⁵ Copy number alterations were assayed in all samples by performing aCGH with microarrays, called submegabase resolution tiling arrays. The fabrication, experimental procedure, performance characteristics and validation of this array have been described earlier.^{14,16} This tiling array contains 97 299 elements, representing 32 433 bacterial artificial chromosome (BAC)–derived amplified fragment pools spotted in triplicate and provide 1.5-fold coverage of the human genome, giving an approximate resolution of 80 kb. Genomic loss, gain and amplification were classified as determined earlier for this platform.¹⁷ The associated breakpoints were identified using the software package *aCGHsmooth* developed by Jong *et al.*¹⁸ (freely available at <http://www.flintbox.ca/technology.asp?tech=FB312FB>). A frequent recurrent abnormality was operationally defined as an abnormal region in >25% of samples.

GEP

Total RNA was extracted with Trizol reagent (Gibco-Invitrogen) and further purified with RNeasy Mini Columns (Qiagen, Valencia, CA, USA). The GEP experiments were performed on GeneChip HG U133 plus 2 (Affymetrix, Inc., Santa Clara, CA, USA), as described earlier.¹⁹ All the raw data from Affymetrix GeneChip were normalized using the BRB-Array Tools,²⁰ and the gene annotation and chromosomal location of each gene was extracted using this tool. GEP data from normal resting and IL-2-activated human NK cells were obtained from our earlier study.¹⁹

Data analysis

The aberrant regions from all cases were aligned to identify the minimal common region in each abnormality, that is, the smallest region that was involved in all the cases with that abnormality. This minimal aberrant region for each abnormal locus was queried/mapped in the human genome database ([www.ncbi.nlm.nih.gov/mapview/Homo sapiens Build 36.1](http://www.ncbi.nlm.nih.gov/mapview/Homo_sapiens_Build_36.1)). The mRNA expression in aberrant genomic regions was first compared among samples with and without the abnormalities and then also compared with normal NK cells (resting and IL-2-activated for 24 h). Genes showing ≥ 2 -fold increase in gained regions or ≥ 2 -fold decreased expression in deleted regions were further analyzed. The transcripts within the gained and deleted regions were clustered using hierarchical clustering and the function of selected genes was identified through the NCBI/OMIM database.

Comparison with previously published data. To compare our findings with previous published data, we assembled all CGH data through an extensive literature search^{4–11,21} that included three studies: conventional CGH on 9 Korean patients,⁴ conventional CGH on 10 Chinese patients⁸ and aCGH on 27 Japanese patients.⁶ We also included other reports

with cytogenetics, loss of heterozygosity (LOH) and fluorescent *in situ* hybridization data on 15 cases of NK-cell malignancies.⁷ The aberrant cytobands or markers were mapped through the human genome database to chromosomal regions as precisely as the data allowed ([www.ncbi.nlm.nih.gov/mapview/Homo sapiens Build 36.1](http://www.ncbi.nlm.nih.gov/mapview/Homo_sapiens_Build_36.1)), and the information entered into an excel file for comparison with our aCGH data. The aberrant regions were aligned to identify the minimal common region of each abnormality.

Quantitative Real-Time RT-PCR, mutational and methylation analysis of PRDM1, ATG5 and AIM1

Quantitative RT-PCR. The expression of three candidate genes in 6q21, (*ATG5*, *AIM1* and *PRDM1 α* (*Blimp1 α*)) was determined by quantitative reverse transcriptase-PCR (qRT-PCR) in all cell lines and in normal NK cells as described earlier¹⁹ (Primers are shown in the Supplementary Table 2).

Mutation analysis. *PRDM1* and *ATG5* cDNA sequences spanning the entire coding region from eight NK cell lines were analyzed for mutation as described earlier.²² If cDNA sequencing revealed a nucleotide difference from previously published wild-type sequence, the corresponding genomic region was sequenced for confirmation. As *AIM1* is a very large gene, we only sequenced conserved coding regions, on the assumption that these are the most functionally important regions and more likely to be targeted by mutations that alter function (Primers are shown in the Supplementary Table 3).

Methylation analysis. In all, 500 ng of genomic DNA was treated with bisulfite using the EZ DNA Methylation-Gold kit (Zymo Research, Orange, CA, USA). Methylation-specific PCR was then performed to survey the methylation status of the CpG islands located at the *ATG5* and *AIM1* promoter regions as described earlier²³ (Primers are shown in the in Supplementary Table 4a).

To more thoroughly analyze the methylation status of multiple CpG sites in the CpG islands, found to be methylated by methylation-specific PCR, each of these regions was subjected to bisulfite sequencing, as performed earlier²⁴ (Primers are shown in the Supplementary Table 4b). The CpG islands in the *PRDM1* gene were sequenced without prior survey. Ten individual insert sequences were analyzed and combined to determine the final methylation percentage at each CpG site.

Western blotting. In all, 25 µg of whole-cell extract from exponentially growing U266 (positive control), KHYG1, NK92, KAI3, SNK6, YT, NKYS was resolved by 10% sodium dodecyl sulfate–polyacrylamide gel electrophoresis and transferred to a polyvinylidene difluoride membrane (GE Healthcare Bio-Science, NJ, USA). The membrane was first blocked in 5% milk/phosphate-buffered saline-T at room temperature for 1 h and then incubated with primary PRDM1 antibody (Clone ROS²⁵) at 4 °C overnight, followed by treatment with horse-radish peroxidase-linked secondary antibody. The immunocomplexes were visualized by enhanced chemiluminescence (ECL Plus) kit (GE Healthcare Bio-Science, NJ, USA) as per the manufacturer's instruction. Detection of α -tubulin was performed to ensure equivalent protein loading.

Treatment of cell lines with DNA methyltransferase inhibitor (Decitabine). Three cell lines (SNK6, KHYG1 and NKYS) with different methylation and deletion status and

transcript levels were chosen for Decitabine treatment. Cells were grown, as described above, in the absence or presence of graded concentrations of Decitabine for 96 h. Cell viability was determined by ATP quantitation using Cell Titer-Glo Luminescent cell viability assay (Promega Inc., WI, USA). Total RNA was extracted (if cell viability is > 50%) and qRT-PCR for *PRDM1α* was performed.

Results

Cell line and patient characteristics

The key characteristics of the cell lines and clinical samples used in the study are summarized in Supplementary Table 1. The cell lines are phenotypically similar to the original neoplasm and only the KHYG1 cell line derived from ANKL was Epstein-Barr Virus (EBV) negative.

The median age of the seven clinical cases was 57 years (range 42–72), and six of these patients were diagnosed with ENKL and one with ANKL, which was the only EBV-negative case. Immunophenotyping of frozen tissue sections revealed no expression of pan-T-cell markers CD3 (Leu4), CD4 and CD5, and no reaction with B-cell markers (Supplementary Table 1b).

Genomic imbalances by aCGH

The aCGH findings are summarized in Figure 1 and Table 1a. Regions previously reported to have natural copy number variation were not included, and we restricted our analysis only to somatic alterations (Database of Genomic Variants, <http://projects.tcag.ca/variation/>).²⁶ There was a higher frequency of deletions than gains. As expected, more chromosomal aberrations were observed in cell lines with an average of 12 losses (range 6–18) and 10 gains (range 3–23) vs an average of 7 losses (range 3–9) and 7 gains (range 4–8) in primary tumor specimens. The most frequent abnormal regions in all tested samples were deletion in 6q21 (60%; 9 of 15), 17p11.2–p13.1 (47%; 7 of 15) and gain in 1q31.3–qter (53%; 8 of 15) and 20pter–qter (47%; 7 of 15). Gains in 1q31.3–qter, 17q21.31–q21.33, 17q23.2–q24.1

and 20pter–qter, and losses in 6q21, 7p14.1, 7p15.3–p22.3, 9p21.3–p22.1, 13q14.11 and 17p11.2–p13.1 were observed in at least two tumor samples (~28%). A few aberrant regions observed in cell lines (for example, gain of 1q21.1–q23.3, loss of 9q13–q21.11; 12q24.31–q24.33; 18q11.1–q12.1 and 18q12.3–qter) have not been reported or are rarely observed in previous studies (Table 1a). Therefore, these aberrations are likely cell line related and they are not further considered in this study.

Comparison with genomic imbalances reported in the literature

The minimal common regions of the frequent aberrations in this study and abnormalities reported earlier are shown in Table 1b. We observed a higher degree of concordance between our aCGH data and those reported by Nakashima *et al*.⁶ Regions of gains observed in at least two previous reports and in our study were bolded in Table 1b. Several gains (for example, 2p23.1–p25.3, 8q21.2–q22, 11q12.2, 14q11.1 and 19p13.3) were only observed in our study but they were observed in both cell lines and NK-cell tumor samples.

Several studies of LOH^{7,10,21} showed consistent loss regions in 6q, 7p, 11q, 13q and 17p, and conventional cytogenetics have shown deletions of 6q, 13q and 17p.^{7,10} Among these, deletions of two regions in 6q (6q21 and 6q25.3) have been consistently observed (6 out of 7 reports) including our study. Deletions that have been also observed in at least three previous studies were bolded (Table 1b). A few losses (for example, 16q13.13, 16q22.2 and 18p11–p11.31) were observed at higher frequency in our study, but more associated with cell lines.

Recurrent genomic gains or losses and their impact on gene expression profiles

In general, the chromosomal aberrations modified the expression of genes residing within the affected regions. However, only 30–50% of the genes in the common minimal regions with gains showed overexpression (≥ 2 fold) (Figure 2a), and similar results were observed for genes residing in regions of losses

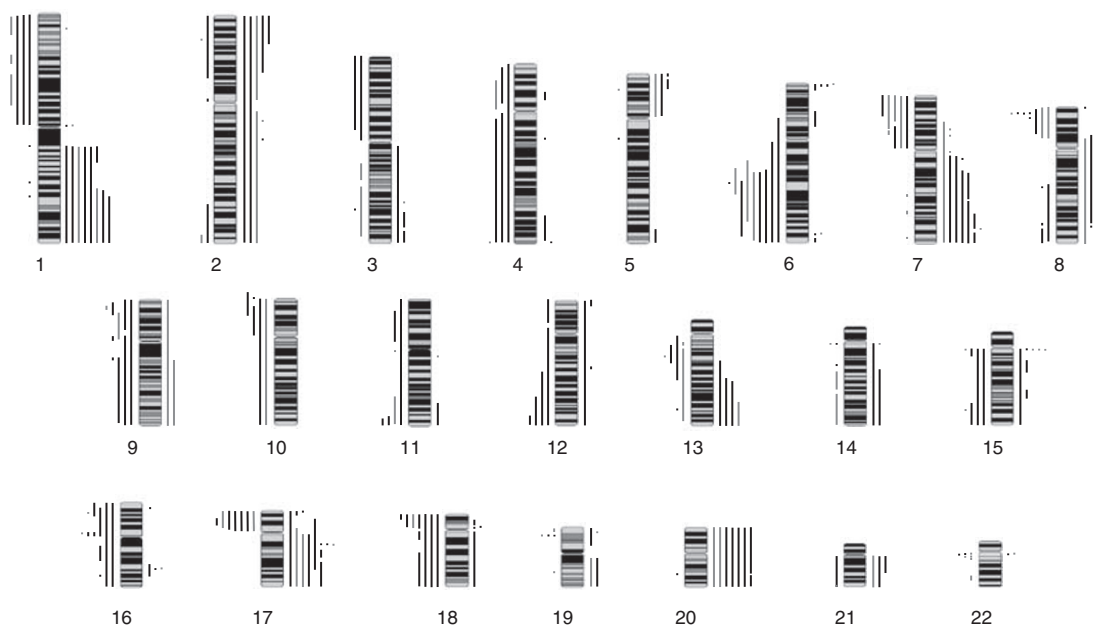


Figure 1 Ideogram representing gains or losses in NK-cell malignancies. Lines on left of each ideogram represent loss and right represent gain. Dark bar indicates cell line and grey bar indicates patient sample.

Table 1a Minimum aberrant regions identified by aCGH for abnormalities with $\geq 25\%$ frequency

Gain(+)/ loss(-)	Common region Band	Base pair start	Base pair end	Cell lines								Tumor specimen							
				KHYG1	NK-92	SNK-1	SNK-6	NK-YS	HANK-1	YT	KAI3	NK01	NK02	NK03	NK04	NK05	NK06	NK07	
+	1q21.1–q23.3	143 032 741	161 714 846			x	x	x			x	x							
+	1q31.3–qter	196 910 109	246 608 256			x	x	x	x		x	x						x	x
+	2p23.1–pter	640 765	30 901 946				x	x	x										
+	7q11.11–q31.1	83 114 648	111 851 165	x	x		x	x				x							
+	7q32.1–q34	126 932 281	143 131 253	x	x		x	x			x		x						
+	7q35–qter	147 152 251	158 777 885	x	x		x	x			x		x						
+	13q31.2–qter	88 504 640	114 117 194	x							x	x	x						
+	17q21.31–q21.33	39 279 823	47 504 844	x				x			x	x	x						
+	17q23.2–q24.1	51 913 051	60 370 955	x				x			x	x	x						
+	20pter–qter	271 054	62 435 964	x			x	x	x		x				x			x	
–	1p36.11–p36.32	655 703	24 150 764			x	x					x		x					
–	1p32.3–p34.1	44 336 255	55 230 951			x	x					x		x					
–	1p21.3–p31.2	66 039 368	98 873 076			x	x					x		x					
–	6q21	105 616 290	107 566 662			x	x	x	x		x	x			x	x			x
–	7p15.3–p22.3	1 499 748	23 381 321		x				x				x	x					
–	7p14.1	38 135 385	42 828 509		x						x		x						
–	9p21.3–p22.1	19 586 561	24 032 423	x			x					x		x				x	
–	9p11.2–p13.1	38 963 616	44 492 799	x							x	x		x					
–	9q13–q21.11	66 653 164	70 224 724	x	x						x	x							
–	10p12.1–p14	7 756 695	25 742 346	x	x	x									x				
–	11q24.2–q25	127 376 748	133 194 384	x				x					x						
–	12q24.31–q24.33	121 598 485	131 701 464		x						x	x							
–	13q14.11	39 236 837	40 287 518					x			x			x					x
–	15q25.3	83 742 222	84 069 794					x			x	x							
–	16p13.13–p13.2	10 308 502	11 853 930			x	x				x	x			x				
–	17p11.2–p13.1	8 633 350	16 294 514		x	x	x				x	x	x			x			
–	18p11.31–pter	35 421	6 245 526	x	x	x	x	x				x		x					
–	18q11.1–q12.1	16 764 897	25 827 987			x	x				x	x							
–	18q12.3–qter	39 758 711	76 098 439			x	x				x	x							

Abbreviation: aCGH, array comparative genomic hybridization.

Table 1b Comparison with previously published data

Chromosomal location	Frequency (%)							
	Cell line	Samples	Ref # 6	Ref # 8	Ref # 4	Ref # 7	Ref # 20	Ref # 11
<i>Recurring gains</i>								
1q21.1	62.5	14.3	30	10				
1q23.1–q23.3	62.5	14.3	30	20				
1q31.3–q32.1	75	28.5	50	10				
1q32.2–q41	75	28.5	50					
1q41–q42.1	75	28.5	50					
1qter–q41	74	28.5	50					
2p16.3–p21	37.5	14.3	17					
2q13–q14	25	28.5	24		28.6			
2q31.1–q32.2	25	14.3	24		42.8			
6p25.2–p25.3	37.5	14.3	40					
7q11.2	37.5	14.3	24	20				
7q21.13–q21.3	50	14.3		20				
7q31.1–q31.2	50	14.3	24	20				
7q35	50	28.5		40				
16q22.2	25	14.3		20				
17q21.1	62.5	43		40	28.6			
20q11.1	62.5	28.5		50				
21q11.2–q22.11	25	14.3			28.6			
<i>Recurring losses^a</i>								
1p36.32	37.5	14.3	58		57			
1p36.23–p36.31	37.5	14.3	30					
1p32.3–34.1	37.5	14.3		28	28.6			
1p21.3–p22.3	37.5	14.3		10				
3q21.3	-	14.3	30					
6q21	62.5	43	35	20		31	100	80
6q23.2	62.5	28.5	47	20				
6q25.3	62.5	14.3	29	30		67	58	
6q26	62.5	14.3	35	10		46		
7p22.1	25	43.5	40	10				
9p22.1–p22.3	37.5	43.5		10				
9cent–p23	37.5	14.3		10				
10p14–p15	37.5	14.3		10				
11q23.1	12.5	14.3	29	20		31		
11q24.3–q25	37.5	14.3		20				
13q14.11	25	28.5		25	14.3	60		
13q14.11–q14.2	12.5	14.3		30				
15q13.1	37.5	14.3	29					
17p13–p13.1	62.5	28.5	40	20	43	40		

Abbreviation: CGH, comparative genomic hybridization.

The 'chromosomal location' shown reflects the minimal common region (MCR) compiled from all the studies and may not be identical to the MCR derived from our study.

^aReferences 6, 8 and 4 include CGH data and other references include LOH data on selected chromosomes e.g. ref. 7 on Chromosome 6, 11, 13 and 17 and ref.s 8 and 9 on chromosome 6 only. Only references with at least 5 cases are included in the table.

Bold: recurrent abnormalities observed in at least two (gains) or three (losses) previous studies.

(Figure 2b). Among the gains, the majority of genes showing overexpression (>2 fold) play a role in cell proliferation, cell cycle progression and metabolic processes. Many of the transcripts were also involved in nucleotide biosynthesis, transcriptional and translational processes, in the secretory pathways, in intracellular protein trafficking, and in mitochondrial transcriptional machinery (Supplementary Table 5a). Unexpectedly, two putative tumor suppressor genes, *AIM2* (1q21.3) and *PHB* (17q21) also showed increased expression. *PHB* interacts with RB and is involved in the repression of E2F-mediated transcription,²⁷ and *AIM2* has been shown to suppress the proliferation and tumorigenicity of human breast cancer cells.²⁸

Within the most frequently loss regions, we observed down-regulation of major functional group of genes including tumor suppressors (*MAP2K4*, *CDKN2C*, *CDKN2A*, *CHFR* and *FOXO1A*), negative regulators of cell cycle or cytoskeleton organization in cell division (*KIF2C*, *MAD2L2* and *MCM10*),

pro-apoptotic genes (*SH3GLB1*, *PRKACB*, *DFFA* and *P53AIP1*) and several transcriptional repressors (*PRDM1α*, *NCOR1* and *ZNF10*) (Supplementary Table 5b). Interestingly, many of the genes, overexpressed in regions of gain, were also observed to be overexpressed in activated NK cells compared with normal resting NK cells. On the other hand, genes in regions of loss were often more highly expressed in resting NK cells compared with activated NK cells.

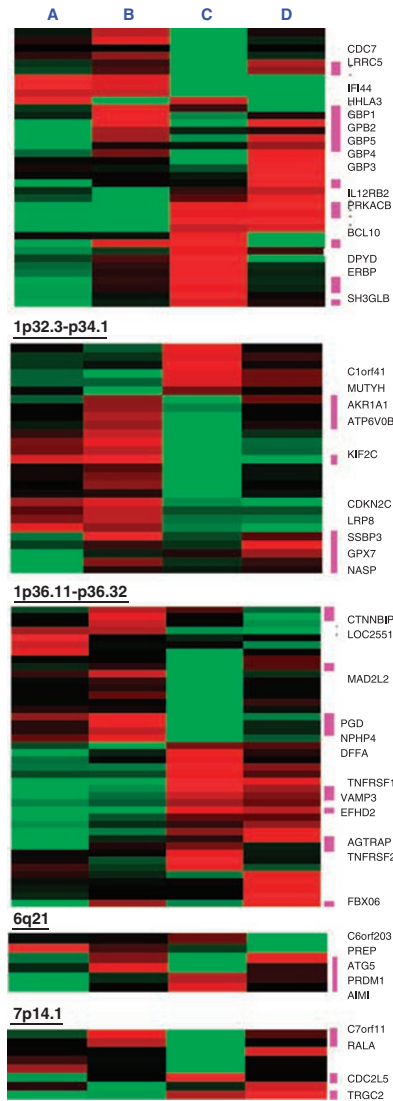
Del 6q21 and expression of ATG5, PRDM1 and AIM1

There are three known genes (*PRDM1*, *ATG5* and *AIM1*) in the minimal region in del 6q21 that generally show low expression in microarray data (Supplementary Figure 1). We analyzed the expression of these genes by qRT-PCR in all the cell lines and showed good correlation with the microarray results (Figures 4a, b and c (ii) and Supplementary Figure 1). *ATG5* showed consistent relatively lower expression (≥2 fold) in all del6q21

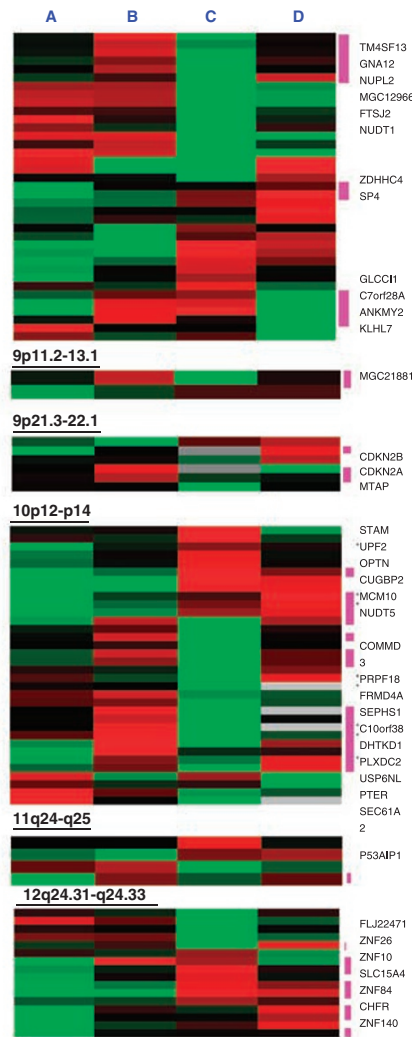


Figure 2 Correlation of genomic aberration with gene expression. Recurrent genomic gains (a) or losses (b) and their gene expression profiles are shown. The median gene expression in cases with (column A) or without genomic aberration (column B), and normal resting (column C) and IL-2-activated (24 h) NK cells (column D). The minimal common region of each abnormality is shown. Genes showing > 2-fold difference between columns A and B are indicated by the blue bars in regions with gain (upregulated genes) and purple bars in regions with loss (downregulated genes). The color in each row represents the gene expression level according to the scale bar shown in the figure. The genes in each region are clustered using a hierarchical clustering program and do not correspond to their location on the chromosome.

b 1p21.3-p31.2



7p15.3-p22.3



13q14

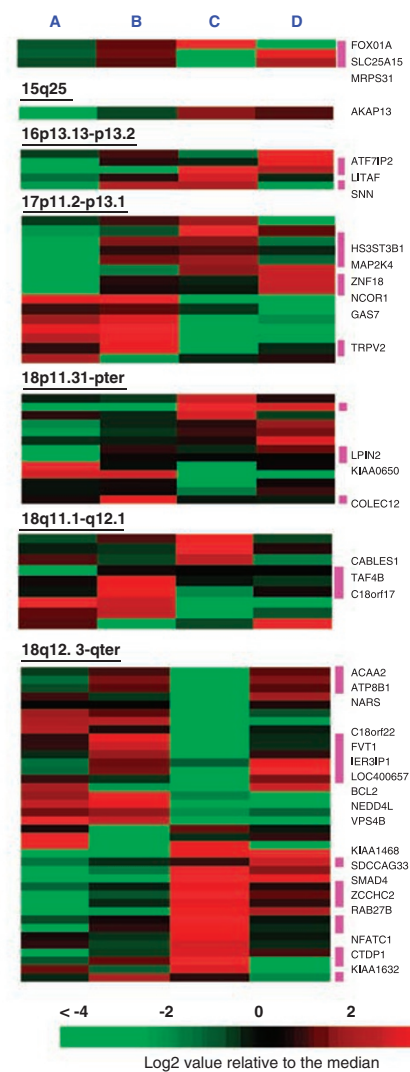


Figure 2 Continued.

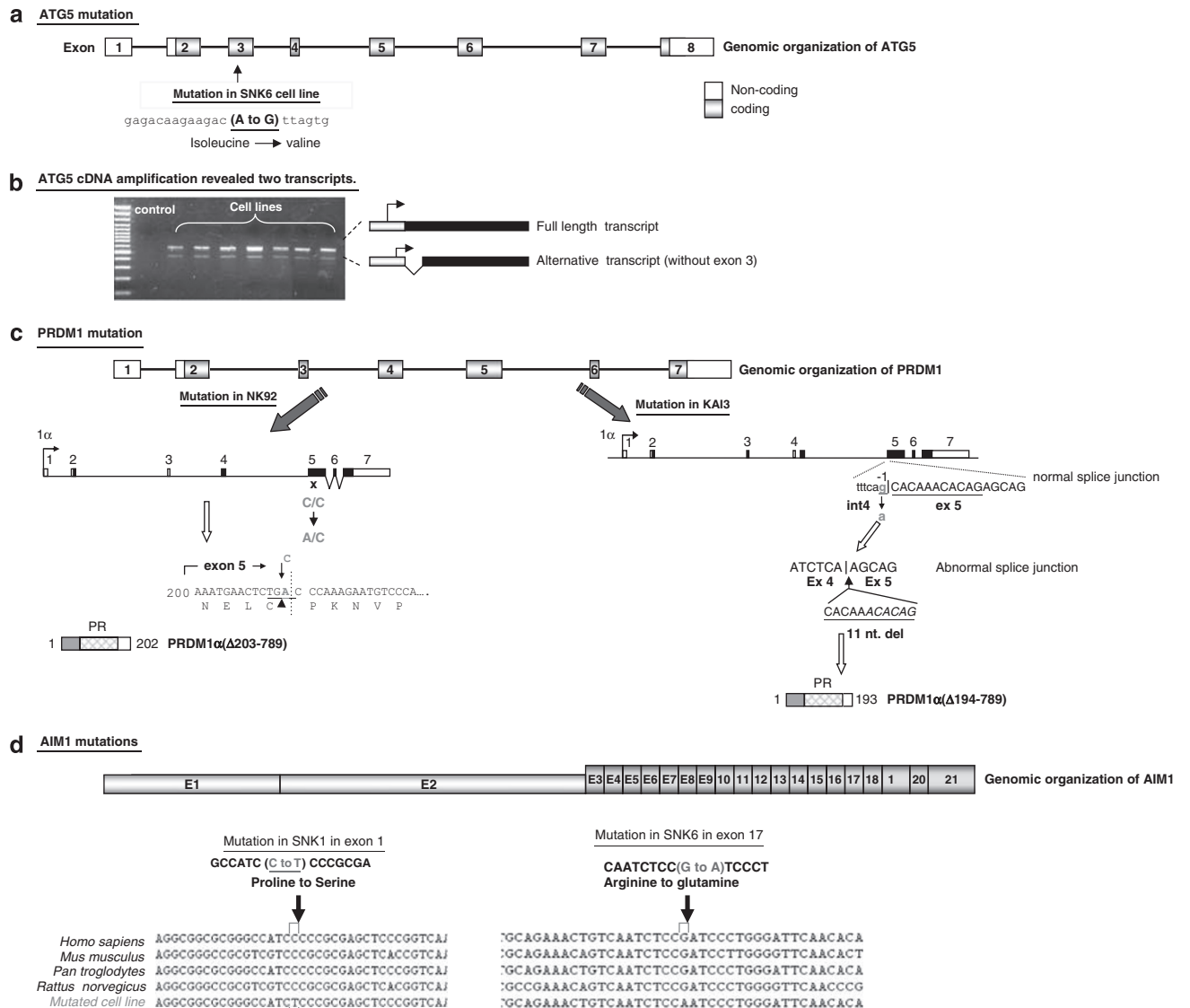


Figure 3 Mutation analysis of *ATG5*, *PRDM1* and *AIM1*. (a) A schematic diagram of *ATG5* illustrating an A→G mutation in exon 3 in SNK6. (b) Two transcripts are expressed including an alternative *ATG5* transcript without exon 3. (c) In NK92, the C→A mutation (bold) results in the generation of a premature translation stop codon (underlined). In KAI3, there is a point mutation (bold) in the consensus splice acceptor sequence at the intron 4/exon 5 junction resulting in the use of a cryptic splice acceptor site further downstream with deletion of an 11 bp sequence (underlined). Predicted structures of the truncated PRDM1 are shown. (d) Sequencing of the conserved coding region in *AIM1* showed point mutations in SNK1 and in SNK6 that result in amino-acid changes.

cell lines than *AIM1* and *PRDM1* (generally ≥ 1.5 fold). The microarray measured the transcription levels of both isoforms of *PRDM1* (*PRDM1 α* and β). Therefore, we specifically measured the expression of the functional isoform (*PRDM1 α*) by qRT-PCR in both neoplastic and normal NK cells. Unexpectedly, *PRDM1 α* expression in KHYG1 cell line (no del6q21) was very low, whereas KAI3 cell line (with del 6q21) showed very high expression (Figure 4b-ii). Western blot analysis of PRDM1 in cell lines detected protein expression only in NKYS cell line (del q21) (Figure 4b-iii). No or very low protein expression was detected in KAI3, YT, KHYG1, NK92 and SNK6 cell lines. The mRNA expression of *PRDM1 α* was low in resting NK cells and at 2 h after culture in IL-2, but the level increased substantially by 8 and 24 h of culture (Supplementary Figure 2).

Mutational analysis of *ATG5*, *PRDM1* and *AIM1*

Sequence analysis of *ATG5* showed only one mutation in the nonconserved coding region of exon 3 (position 487; A→G) in SNK6 resulting in an amino-acid change from isoleucine to valine (Figure 3a). An alternative shorter transcript was detected in all cell lines resulting from alternative splicing that deleted exon 3 (Figure 3b). *PRDM1* showed a C→A nonsense mutation in exon 5 in NK92 cell line (no del 6q21) and a G→A point mutation at the consensus splice acceptor sequence at the intron 4/exon 5 junction, in KAI3 (with del 6q21). Both of these mutations resulted in truncated proteins with loss of function (Figure 3c). Western blotting confirmed the absence of wild-type PRDM1 α in KAI3 (Figure 4b-iii).

The analysis of the conserved coding regions of *AIM1* showed mutation in exon 1 (C→T) and exon 17 (G→A) in SNK1 and

SNK6 cell lines, respectively, resulting in corresponding amino-acid changes (Figure 3d). These mutations were also detected in the corresponding genomic DNA.

Methylation analysis of *ATG5*, *PRDM1* and *AIM1*

The sequence within +1 to -3.5 Kb of the transcription start site (TSS) of *AIM1*, *ATG5* and *PRDM1* were screened for enriched CpG regions by the UCSC genomic browser (<http://genome.ucsc.edu/>). Methylation-specific PCR analysis on *ATG5* promoter showed little methylation in two CpG islands close to the TSS (+568 to -110bp), but extensive methylation of the SINE (-477 to -751 bp) and LTR region (~-2.1 to -3.1 Kb) as expected (Supplementary Figure 3a). These results were confirmed by sequencing on bisulfite-treated DNA at the SINE region and the region between +568 to -110bp of the TSS. Methylation at the SINE region did not correlate with either deletion status or transcription level of the *ATG5* gene (Figure 4a (i,ii)).

For *PRDM1* (-260 to +250), the CpG-rich region, 200–250bp upstream of the TSS was almost fully methylated in KHYG1 (70–100%), but less methylated in NK92 (50–60%). Among the 6q21-deleted cell lines, SNK1 and SNK6 showed extensive methylation at the same CpG locus (70–100%). Correlation with mRNA expression suggested a significant association of methylation with lower expression of *PRDM1* in KHYG1, SNK1 and SNK6 (Figure 4b (i-ii)). Western blotting analysis in KHYG1, NK92 and SNK6 also revealed the absence or very low expression of wild-type PRDM1 (Figure 4b-iii).

Methylation-specific PCR analysis of *AIM1* showed methylation 5' to the TSS (-980 to -1360) in five cell lines (HANK1, YT, NKYS, SNK1 and KHYG1) and 3' of TSS (+30 to +380) in two cell lines (HANK1 and YT) (Supplementary Figure 3b). Sequencing on bisulfite-treated DNA provided a more detailed pattern of methylation in HANK1, SNK1 and YT (Figure 4c). Scattered methylated sites 3' of TSS (50–60%) were detected in HANK1 ($n=15$, +173 to +336) as well as in SNK1 ($n=7$; +205 to +303) but not seen in YT. Both HANK1 and SNK1 showed lower *AIM1* mRNA expression than other 6q21-deleted cell lines (Figure 4c i,ii).

Treatment of NK cell lines with Decitabine

The treatment of two cell lines with methylated promoter (SNK6 and KHYG1) with Decitabine showed >2-fold increase in *PRDM1* mRNA level (Figure 5a). In contrast, NKYS, a cell line without methylated promoter, showed no significant increase in *PRDM1* mRNA level even with high concentrations of Decitabine. Interestingly, the cell lines (SNK6 and KHYG1) with methylated promoter showed significant cytotoxic effect on Decitabine treatment, while NKYS was resistant (Figure 5b).

Discussion

NK-cell malignancies encompass a spectrum of presentation and are among the most aggressive lymphoid malignancies.²⁹ Like other hematological malignancies, they are associated with

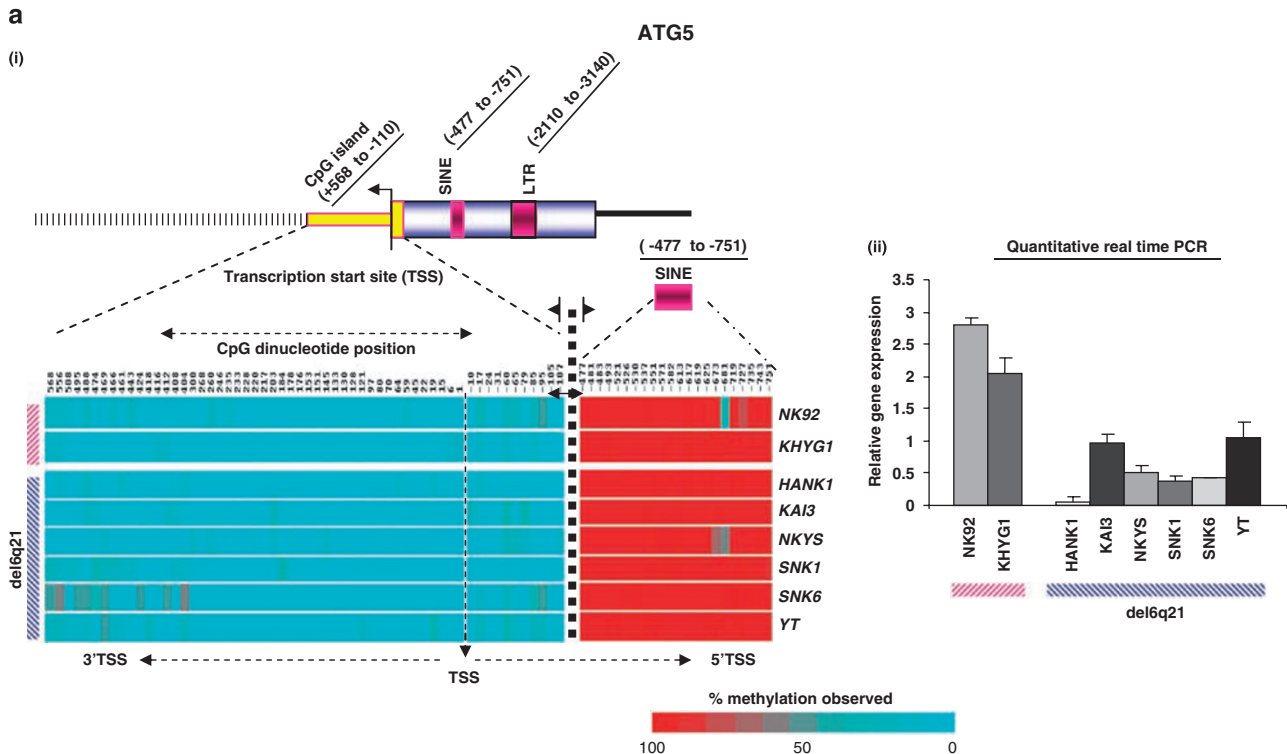


Figure 4 Methylation analysis of *ATG5*, *PRDM1* and *AIM1*. (a) (i) Bisulfite sequencing of *ATG5* revealed high methylation in the SINE region, but minimal methylation in the CpG islands 3' and 5' of TSS. (ii) No association of *ATG5* expression with methylation. (b) (i) Methylation analysis of *PRDM1* revealed high methylation (60–100%) in the 5' region of the CpG island in KHYG1, SNK1 and SNK6, and lower methylation (50–60%) in NK92. (ii) qRT-PCR showed significant association of *PRDM1*a expression with methylation in this site. (iii) Western blot analysis of *PRDM1* in myeloma cell line (U266, as positive control) and NK cell lines using antibody to the N terminus of *PRDM1*. *PRDM1* was detected in U266 and NKYS only and was absent or having very low expression in other NK cell lines. (c) (i) Bisulfite sequencing of *AIM1* showed highly methylated CpG island in HANK1, NKYS, SNK1 and YT 5' to the TSS and additional methylation sites in the CpG island 3' to the TSS in HANK1, YT and SNK1 (ii) low expression of *AIM1* in HANK1 and SNK1, but not in YT. TSS, transcription start site; qRT-PCR, quantitative reverse transcriptase-PCR.

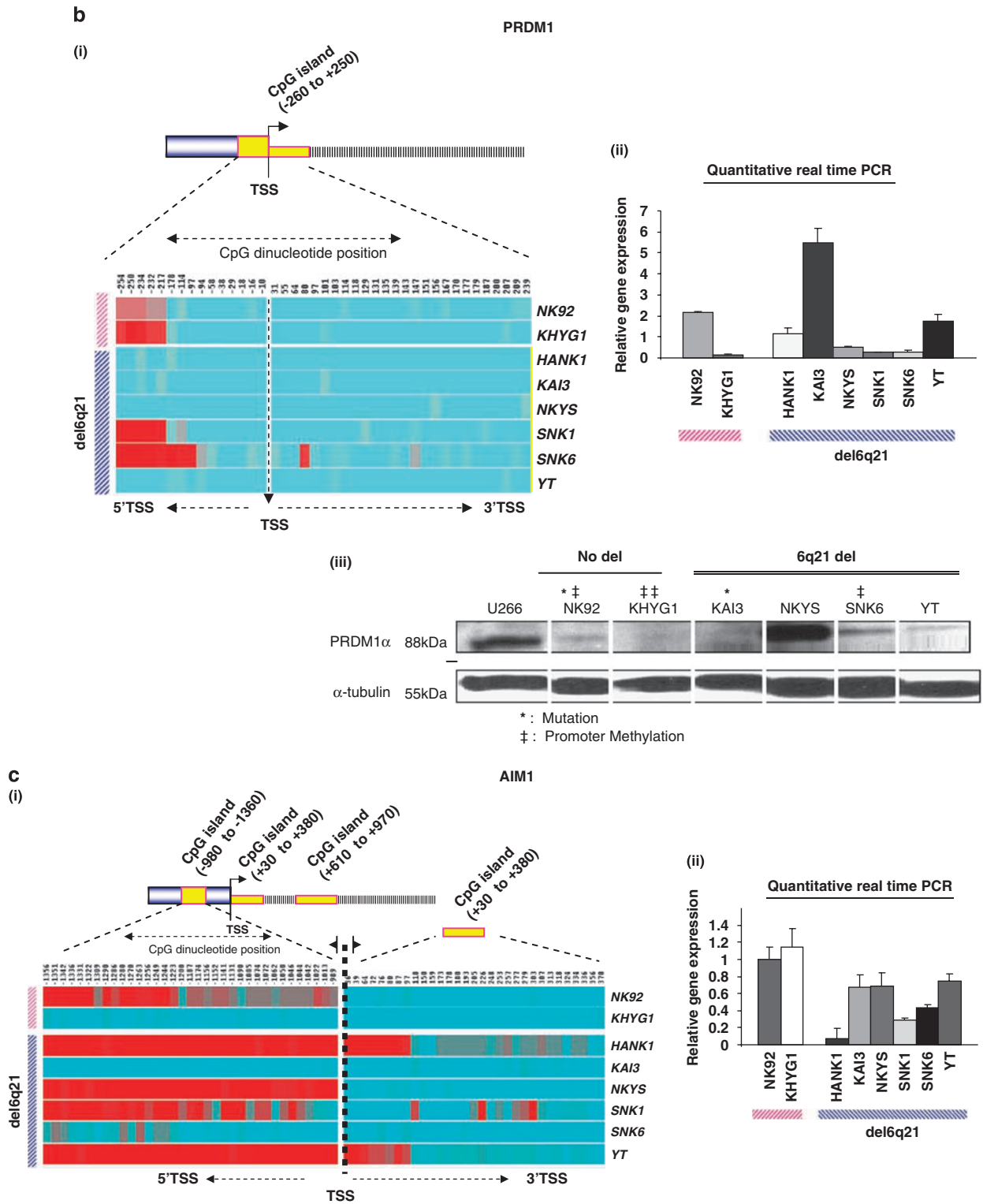


Figure 4 Continued.

certain frequently occurring karyotypic abnormalities,^{30,31} and these chromosomal aberrations are important in the pathogenesis and tumor evolution. These aberrations are strongly selected, and are preserved even after years of cell culture.^{32,33} It is logical to speculate that the functional consequence and presumed selective advantage of these chromosomal aberrations

are exerted through modifications of the expression of certain genes residing in or close to these aberrations. In this study, we examined the frequency of genomic abnormalities in a panel of well-characterized malignant NK cell lines and clinical specimens to determine the impact of these abnormalities on the expression of genes residing in these regions.

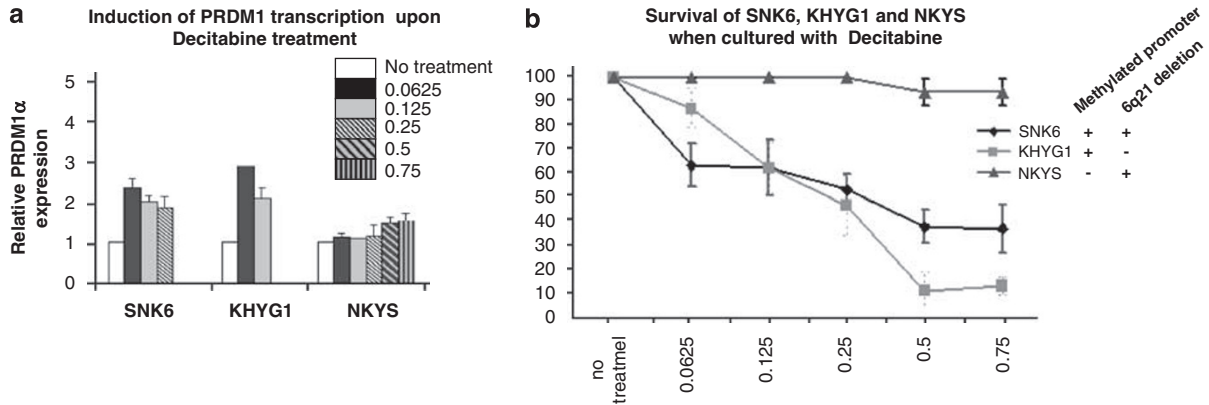


Figure 5 *PRDM1a* expression and cell survival after Decitabine treatment: **(a)** qRT-PCR shows upregulation of *PRDM1a* in SNK6 and KHYG1 after Decitabine treatment. **(b)** SNK6 and KHYG1, but not NKYS are sensitive to Decitabine. qRT-PCR, quantitative reverse transcriptase-PCR.

Most of the frequent gains and losses in the present study showed good concordance with previous studies, although the frequencies are quite variable from study to study. Nakashima *et al.*⁶ showed differences between the genomic imbalances of ANKL and ENKL. They found that gains of 1q23.1–q24.2 and 1q31.3–q44, and loss of 7p15.1–p22.3 and 17p13.1 occurred more often in the former. Abnormal regions found preferentially in ENKL were gains of 2q11.2–q37, and losses of 6q16.1–q27, 11q22.3–q23.3 and 4q31.3–q32.1.⁶ We did not attempt to divide our cases into subcategories of NK-cell malignancies due to the small number of samples, but instead focused on abnormalities that are commonly present and probably important in the pathogenesis of NK-cell malignancies. Consolidating data from other studies^{4,6,8} points to gains in 1q, 7q35, 17q21.2 and 20q11.1 are the most frequent. We examined the expression of > 1000 transcripts residing in these regions and found that generally 30–50% of genes in these aberrant regions showed increase in expression compared with cases without the gains. An examination of the functions of upregulated genes suggests that the selective advantage of chromosomal gains derives at least partially from the upregulation of genes supporting the dysregulated cellular proliferation and growth required for tumorigenesis. The increased expression of genes associated with mitochondrial protein synthesis may indicate the need to supply extra energy in relation to the above processes. In general, the expression of these genes was also significantly higher in activated NK cells (after 24 h of IL-2 culture) compared with normal resting NK cells consistent with the role of these genes in NK-cell activation, growth and proliferation. However, there is a significant difference in the profile of upregulated genes in malignant NK cells compared with the activated normal counterpart. The differential gene expression may offer some insight into the abnormal regulation of proliferation, growth and metabolism in the neoplastic cells.

When we examine downregulated genes in deleted regions, we observed several important functional alterations that alone or in cooperation with the abnormal gene expression in regions of gain may contribute to neoplastic transformation. A frequent loss in 9p22.1–p22.3 includes known tumor suppressor genes *CDKN2B* (*p15INK4B*) and *CDKN2A* (*p16INK4A*) that were downregulated in deleted cases. There are other genes with low expression in deleted regions that are involved in cell-cycle control (for example, *CDKN2-A*, *-B*, *-C*, *MCM10*, *CDC7* and *MADL2*) and in maintaining cell quiescence (for example,

*FOXO1A*³⁴ and *LITAF*). *FOXO1A* is located in a commonly deleted region in 13q14.11. The normal functions of these genes may be disturbed by the deletion with or without accompanying abnormalities of the remaining allele, leading to impaired control of cellular activation and the cell cycle.

Although *TP53* may be lost in del17p, the *TP53* locus may not be included in the region 17p11.2–p13.1 that is frequently involved. This is consistent with some previous LOH studies.^{7,35} Thus, there may be important tumor suppressor genes other than *TP53* in this region. We observed downregulation of transcripts including *GAS7*, *HS3ST3B1*, *MAP2K4*, *ZNF18* and *NCOR1*. *ZNF18* and *GAS7* are uncharacterized transcription factors, whereas *NCOR1* is a transcription co-repressor that may be involved in the repression of a subset of nuclear factor-κB-regulated genes³⁶ and inhibition of the Jun N-terminal kinase pathway.³⁷ *MAP2K4* (*MKK4*) has been implicated as a metastasis suppressor gene.³⁸ 7p22.1 was frequently deleted and associated with downregulation of transcription factors *ZDHHC4*, *ANKMY2* and *SP4*. Thus, a number of transcription regulators and putative tumor suppressor genes are implicated in the deleted regions and their role in the pathogenesis of NK malignancies remains to be determined.

Del 6q was the most frequent loss as in earlier studies^{4,6,8} and four distinct regions: 6q21, 6q23.2, 6q25.3 and 6q26 have been suggested.^{7,10,11,21,39} Previous results and our data suggest that 6q21 (~105.6–107 Mb) is the most common aberrant region (Table 1a). Of the eight known genes in the common minimal region of the 6q21 locus, *ATG5* and *PRDM1* (*Blimp-1*) had the most consistently low expression. Three other genes at this locus, *C6orf203*, *PREP* and *AIM1*, were marginally downregulated (between 2 and 1.5 fold), but only *AIM1* has been implicated in tumor suppression in melanoma.⁴⁰ We, therefore, focused our attention on *ATG5*, *PRDM1* and *AIM1*.

Sequencing and methylation analysis of the remaining *ATG5* allele provided evidence that this allele remains functional and suggest that haplo-insufficiency rather than complete elimination of function may promote tumorigenesis, similar to what has been found for *ATG6* (*BECN1*).⁴¹ *ATG5* is involved in IFN-γ-induced autophagic cell death⁴² and has an important homeostatic role in response to nutrient deprivation. The role of autophagy in carcinogenesis has been somewhat controversial with reports suggesting both tumor-promoting and tumor-suppressing function.⁴³ It is likely that the functional implication of autophagy is context and level dependent. *ATG5* is the first gene in the autophagy pathway to be implicated in lymphoma

and lower but not complete absence of expression may be optimal for survival of NK tumor cells.

We detected occasional *AIM1* mutations that resulted in amino-acid changes in the conserved regions. Methylation in the CpG island 3' to the TSS of the *AIM1* gene was observed in three cell lines (HANK1, YT and SNK1) and was associated with low *AIM1* expression in HANK1 and SNK1. These changes may influence the expression and function of this gene, but *AIM1* is neither structurally nor functionally well characterized and its mechanistic role in NK-cell lymphomagenesis requires further investigation.

PRDM1 is a transcriptional repressor and a master regulator of B-cell differentiation,⁴⁴ and has recently been shown to be important for T-cell homeostasis and self tolerance.⁴⁵ *PRDM1* has been shown to have loss-of-function mutations in 25% of activated B cell-like diffuse large B-cell lymphoma (DLBCL).^{22,46} Our analysis also revealed similar loss-of-function mutations in two cell lines KAI3 and NK92. Thus, both deletion and deleterious mutations of *PRDM1* have now been shown in NK-cell malignancies, but they are not frequently present together. Methylation analysis of the *PRDM1* revealed that a part of the CpG island 5' to the TSS was highly methylated in KHYG1, SNK1 and SNK6. This region encompasses the putative binding site for transcription factors (TFs) GATA1/GATA2 and HSAF1/2. There is no published data that these TFs are involved in the regulation of the *PRDM1* transcription. Also, while methylation of a TF-binding site may affect TF binding, there is still some controversy regarding the universality of this effect.^{47–50} The significance of these TF-binding sites requires further investigation. *PRDM1* expression was very low in all three cell lines with methylation and treatment of cell lines with DNA methyltransferase inhibitor increases the expression of *PRDM1*. This provides further evidence that DNA methylation indeed regulates *PRDM1* expression. Thus, *PRDM1* shows the features of a classic tumor suppressor gene with deletion of one allele and mutation or methylation that inactivate the other allele, and is the most likely target gene of this locus. Surprisingly in KAI3 cell line with del6q21 and mutation of the remaining allele, the abnormal transcript was expressed at a very high level. As no functional protein could be produced and the promoter was not methylated, it is possible that the expression was deregulated due to the lack of some form of negative feedback. *PRDM1α* is expressed in normal resting NK cells at a low level and its level rises substantially by 8 and 24 h of culture in IL-2 (Supplementary Figure 2). It is conceivable that this increase in *PRDM1* level in activated NK cells may be important in NK-cell homeostasis, and disruption of this control may play a role in malignant transformation. In this regard, it is interesting to observe that Decitabine is toxic to cell lines with methylated *PRDM1* promoter but not to an unmethylated cell line. The molecular mechanism of *PRDM1* in NK-cell transformation and its potential as a therapeutic target warrant further investigation.

In conclusion, high-resolution aCGH has helped to more precisely define the boundaries of gains and losses involved in NK-cell malignancies. Concomitant GEP studies allowed us to show that upregulated genes in regions of gain were generally associated with dysregulation of proliferation, growth and change in energy metabolism, suggesting that some of the genomic alterations may provide synergistic functional alterations that promote tumor cell growth and proliferation. This approach also allowed us to narrow down the number of candidate genes in the aberrant regions. The most interesting finding in del 6q21 is the identification of three most likely candidate genes: *PRDM1*, *ATG5* and *AIM1*. Sequencing and methylation analysis suggest that haploid insufficiency of *ATG5*

is the consequence of this deletion. In contrast, both mutations and suppression of transcription by DNA methylation were detected in *AIM1* and *PRDM1* and in the latter, these changes have been shown to contribute to loss of function of the nondeleted alleles as in classical tumor suppressor genes. Although *PRDM1* and *AIM1* have been implicated in the pathogenesis of DLBCL and melanoma, respectively, this is the first study to implicate them in NK-cell malignancies. Similarly, *ATG5* is the first gene in the autophagy pathway to be implicated in lymphoma. Additional studies on larger series of cases will allow us to similarly identify the most likely candidate genes in other commonly affected loci and lead to better understanding of the functional consequences of these genetic aberrations and the molecular oncogenesis of this aggressive lymphoma.

Acknowledgements

This study was supported in part by a NCI Grant (5U01/CA114778) and funds from Genome center Canada/British Columbia. We thank Dr Junjiro Tsuchiyama and Dr Yoshitoyo Kagami for NK-YS and HANK-1 cell lines, respectively. The UNMC Microarray Core Facility Dr James Eudy supported partially by NIH Grant P20 RR016469 from the INBRE Program of the National Center for Research Resources.

References

- Harris NL, Stein H, Vardiman JW (eds). *Pathology and Genetics of Tumors of the Haematopoietic and Lymphoid Tissues*. World Health Organization Classification of Tumors Lyon: International Agency for Research on Cancer, 2001.
- Kwong YL. Natural killer-cell malignancies: diagnosis and treatment. *Leukemia* 2005; **19**: 2186–2194.
- Chan JK. Natural killer cell neoplasms. *Anat Pathol* 1998; **3**: 77–145.
- Ko YH, Choi KE, Han JH, Kim JM, Ree HJ. Comparative genomic hybridization study of nasal-type NK/T-cell lymphoma. *Cytometry* 2001; **46**: 85–91.
- MacLeod RA, Nagel S, Kaufmann M, Greulich-Bode K, Drexler HG. Multicolor-FISH analysis of a natural killer cell line (NK-92). *Leuk Res* 2002; **26**: 1027–1033.
- Nakashima Y, Tagawa H, Suzuki R, Karnan S, Karube K, Ohshima K et al. Genome-wide array-based comparative genomic hybridization of natural killer cell lymphoma/leukemia: different genomic alteration patterns of aggressive NK-cell leukemia and extranodal NK/T-cell lymphoma, nasal type. *Genes Chromosomes Cancer* 2005; **44**: 247–255.
- Siu LL, Chan V, Chan JK, Wong KF, Liang R, Kwong YL. Consistent patterns of allelic loss in natural killer cell lymphoma. *Am J Pathol* 2000; **157**: 1803–1809.
- Siu LL, Wong KF, Chan JK, Kwong YL. Comparative genomic hybridization analysis of natural killer cell lymphoma/leukemia. Recognition of consistent patterns of genetic alterations. *Am J Pathol* 1999; **155**: 1419–1425.
- Wong KF. Genetic changes in natural killer cell neoplasms. *Leuk Res* 2002; **26**: 977–978.
- Wong KF, Chan JK, Kwong YL. Identification of del(6)(q21q25) as a recurring chromosomal abnormality in putative NK cell lymphoma/leukaemia. *Br J Haematol* 1997; **98**: 922–926.
- Yoon J, Ko YH. Deletion mapping of the long arm of chromosome 6 in peripheral T and NK cell lymphomas. *Leuk Lymphoma* 2003; **44**: 2077–2082.
- Suzuki R. Leukemia and Lymphoma of Natural Killer Cells. *J Clin Exp Hematopathol* 2005; **45**: 51–70.
- Snijders AM, Nowak N, Segraves R, Blackwood S, Brown N, Conroy J et al. Assembly of microarrays for genome-wide measurement of DNA copy number. *Nat Genet* 2001; **29**: 263–264.

- 14 Ishkanian AS, Malloff CA, Watson SK, DeLeeuw RJ, Chi B, Coe BP *et al*. A tiling resolution DNA microarray with complete coverage of the human genome. *Nat Genet* 2004; **36**: 299–303.
- 15 Sambrook J, Russell DW. *Molecular Cloning: A Laboratory Manual*, 3rd edn, vol. 1. CSHL Press: Cold Spring Harbor Laboratory Press: Cold Spring Harbor, New York, 2001.
- 16 Watson SK, deLeeuw RJ, Ishkanian AS, Malloff CA, Lam WL. Methods for high throughput validation of amplified fragment pools of BAC DNA for constructing high resolution CGH arrays. *BMC Genomics [Electronic Resource]* 2004; **5**: 6.
- 17 de Leeuw RJ, Davies JJ, Rosenwald A, Bebb G, Gascoyne RD, Dyer MJ *et al*. Comprehensive whole genome array CGH profiling of mantle cell lymphoma model genomes. *Hum Mol Genet* 2004; **13**: 1827–1837.
- 18 Jong K, Marchori E, van der Vaart A, Ylstra B, Weiss M, Meijer G (eds). Chromosomal breakpoint detection in human cancer. In *Applications of Evolutionary Computing. EvoBIO: Evolutionary Computation and Bioinformatics*. Springer LNCS: Springer Berlin/Heidelberg, 2003, pp 54–65.
- 19 Dybkaer K, Iqbal J, Zhou G, Geng H, Xiao L, Schmitz A *et al*. Genome wide transcriptional analysis of resting and IL2 activated human natural killer cells: gene expression signatures indicative of novel molecular signaling pathways. *BMC Genomics [Electronic Resource]* 2007; **8**: 230.
- 20 Simon R, Peng A. *BRB-ArrayTools User Guide*, version 3.6.0. Biometric Research Branch, National Cancer Institute. [cited; Available from: <http://linus.nci.nih.gov/BRB-ArrayTools.html>:Year 2008].
- 21 Ohshima K, Haraokaa S, Ishihara S, Ohgami A, Yoshioka S, Suzumiya J *et al*. Analysis of chromosome 6q deletion in EBV-associated NK cell leukaemia/lymphoma. *Leuk Lymphoma* 2002; **43**: 293–300.
- 22 Tam W, Gomez M, Chadburn A, Lee JW, Chan WC, Knowles DM. Mutational analysis of PRDM1 indicates a tumor-suppressor role in diffuse large B-cell lymphomas. *Blood* 2006; **107**: 4090–4100.
- 23 Radhakrishnan P, Basma H, Klinkebiel D, Christman J, Cheng PW. Cell type-specific activation of the cytomegalovirus promoter by dimethylsulfoxide and 5-aza-2'-deoxycytidine. *Int J Biochem Cell Biol* 2008; **40**: 1944–1955.
- 24 Radhakrishnan P, Basma H, Klinkebiel D, Christman J, Cheng PW. Cell type-specific activation of the cytomegalovirus promoter by dimethylsulfoxide and 5-Aza-2'-deoxycytidine. *Int J Biochem Cell Biol* 2008; **40**: 1944–1955.
- 25 Tam W, Gomez M, Nie K. Significance of PRDM1beta expression as a prognostic marker in diffuse large B-cell lymphomas. *Blood* 2008; **111**: 2488–2489; author reply 2489–2490.
- 26 Wong KK, DeLeeuw RJ, Dosanjh NS, Kimm LR, Cheng Z, Horsman DE *et al*. A comprehensive analysis of common copy-number variations in the human genome. *Am J Hum Genet* 2007; **80**: 91–104.
- 27 Wang S, Nath N, Adlam M, Chellappan S. Prohibitin, a potential tumor suppressor, interacts with RB and regulates E2F function. *Oncogene* 1999; **18**: 3501–3510.
- 28 Chen IF, Ou-Yang F, Hung JY, Liu JC, Wang H, Wang SC *et al*. AIM2 suppresses human breast cancer cell proliferation *in vitro* and mammary tumor growth in a mouse model. *Mol Cancer Ther* 2006; **5**: 1–7.
- 29 Nava VE, Jaffe ES. The pathology of NK-cell lymphomas and leukemias. *Adv Anat Pathol* 2005; **12**: 27–34.
- 30 Wong N, Wong KF, Chan JK, Johnson PJ. Chromosomal translocations are common in natural killer-cell lymphoma/leukemia as shown by spectral karyotyping. *Hum Pathol* 2000; **31**: 771–774.
- 31 Wong KF, Zhang YM, Chan JK. Cytogenetic abnormalities in natural killer cell lymphoma/leukaemia—is there a consistent pattern? *Leuk Lymphoma* 1999; **34**: 241–250.
- 32 Ghadimi BM, Schrock E, Walker RL, Wangsa D, Jauho A, Meltzer PS *et al*. Specific chromosomal aberrations and amplification of the AIB1 nuclear receptor coactivator gene in pancreatic carcinomas. *Am J Pathol* 1999; **154**: 525–536.
- 33 Macville M, Schrock E, Padilla-Nash H, Keck C, Ghadimi BM, Zimonjic D *et al*. Comprehensive and definitive molecular cytogenetic characterization of HeLa cells by spectral karyotyping. *Cancer Res* 1999; **59**: 141–150.
- 34 Medema RH, Kops GJ, Bos JL, Burgering BM. AFX-like Forkhead transcription factors mediate cell-cycle regulation by Ras and PKB through p27kip1. *Nature* 2000; **404**: 782–787.
- 35 Su GH, Hilgers W, Shekher MC, Tang DJ, Yeo CJ, Hruban RH *et al*. Alterations in pancreatic, biliary, and breast carcinomas support MKK4 as a genetically targeted tumor suppressor gene. *Cancer Res* 1998; **58**: 2339–2342.
- 36 Baek SH, Ohgi KA, Koo EH, Glass CK, Rosenfeld MG. Exchange of N-CoR corepressor and Tip60 coactivator complexes links gene expression by NF-kappaB and beta-amyloid precursor protein. *Cell* 2002; **110**: 55–67.
- 37 Zhang J, Kalkum M, Chait BT, Roeder RG. The N-CoR-HDAC3 nuclear receptor corepressor complex inhibits the JNK pathway through the integral subunit GPS2. *Mol Cell* 2002; **9**: 611–623.
- 38 Teng DH, Perry III WL, Hogan JK, Baumgard M, Bell R, Berry S *et al*. Human mitogen-activated protein kinase kinase 4 as a candidate tumor suppressor. *Cancer Res* 1997; **57**: 4177–4182.
- 39 Sun HS, Su IJ, Lin YC, Chen JS, Fang SY. A 2.6 Mb interval on chromosome 6q25.2–q25.3 is commonly deleted in human nasal natural killer/T-cell lymphoma. *Br J Haematol* 2003; **122**: 590–599.
- 40 Ray ME, Wistow G, Su YA, Meltzer PS, Trent JM. AIM1, a novel non-lens member of the betagamma-crystallin superfamily, is associated with the control of tumorigenicity in human malignant melanoma. *Pro Natl Acad Sci USA* 1997; **94**: 3229–3234.
- 41 Qu X, Yu J, Bhagat G, Furuya N, Hibshoosh H, Troxel A *et al*. Promotion of tumorigenesis by heterozygous disruption of the bclm1 autophagy gene. *J Clin Invest* 2003; **112**: 1809–1820.
- 42 Kuma A, Hatano M, Matsui M, Yamamoto A, Nakaya H, Yoshimori T *et al*. The role of autophagy during the early neonatal starvation period. *Nature* 2004; **432**: 1032–1036.
- 43 Hippert MM, O'Toole PS, Thorburn A. Autophagy in cancer: good, bad, or both? *Cancer Res* 2006; **66**: 9349–9351.
- 44 Turner Jr CA, Mack DH, Davis MM. Blimp-1, a novel zinc finger-containing protein that can drive the maturation of B lymphocytes into immunoglobulin-secreting cells. *Cell* 1994; **77**: 297–306.
- 45 Kallies A, Hawkins ED, Belz GT, Metcalf D, Hommel M, Corcoran LM *et al*. Transcriptional repressor Blimp-1 is essential for T cell homeostasis and self-tolerance. *Nat Immunol* 2006; **7**: 466–474.
- 46 Pasqualucci L, Compagno M, Houlisworth J, Monti S, Grunn A, Nandula SV *et al*. Inactivation of the PRDM1/BLIMP1 gene in diffuse large B cell lymphoma. *J Exp Med* 2006; **203**: 311–317.
- 47 Iguchi-Aruga SM, Schaffner W. CpG methylation of the cAMP-responsive enhancer/promoter sequence TGACGTCA abolishes specific factor binding as well as transcriptional activation. *Genes Dev* 1989; **3**: 612–619.
- 48 Maier H, Colbert J, Fitzsimmons D, Clark DR, Hagman J. Activation of the early B-cell-specific mb-1 (Ig-alpha) gene by Pax-5 is dependent on an unmethylated Ets binding site. *Mol Cell Biol* 2003; **23**: 1946–1960.
- 49 Harrington MA, Jones PA, Imagawa M, Karin M. Cytosine methylation does not affect binding of transcription factor Sp1. *Pro Natl Acad Sci USA* 1988; **85**: 2066–2070.
- 50 Holler M, Westin G, Jiricny J, Schaffner W. Sp1 transcription factor binds DNA and activates transcription even when the binding site is CpG methylated. *Genes Dev* 1988; **2**: 1127–1135.

Supplementary Information accompanies the paper on the Leukemia website (<http://www.nature.com/leu>)